REP RTS

major determinant of toxicity[10, 11]

bacterial cells remained constant during the entire culture period in the presence of DON or 3A-DON (Fig. 2A). These results indicate that S3-4 cells grew slowly and retained high DON degradation activity under oligotrophic culture conditions.

To evaluate the ability of S3-4 to degrade DON in agricultural products, wheat grains infected with *F. graminearum* and contaminated with DON were ground, incubated with S3-4 and monitored by HPLC for DON degradation. Wheat samples contained 112 µg of DON before treatment, and after incubation with S3-4 for 72 hours, no DON was detectable (Fig. 2B). In contrast, levels of DON in control samples that were incubated in MM without S3-4, were not significantly reduced after 72 hours. These results demonstrate that strain S3-4 can completely eliminate DON from wheat.

To detect the products of DON degradation, metabolites from S3-4 cultures (100 µg/mL DON) at 0 hai and 120 hai were extracted and analyzed by HPLC. At 120 hai, there were two new compounds with retention times of 7.65 min (compound A) and 3.29 min (compound B), respectively (Fig. 3A). These compounds were produced at different times after inoculation with DON; significant levels of compound A accumulated at 12 hai, then levels sharply increased at 60 hai, and remained high at 120 hai. In contrast, compound B was not detectable until 72

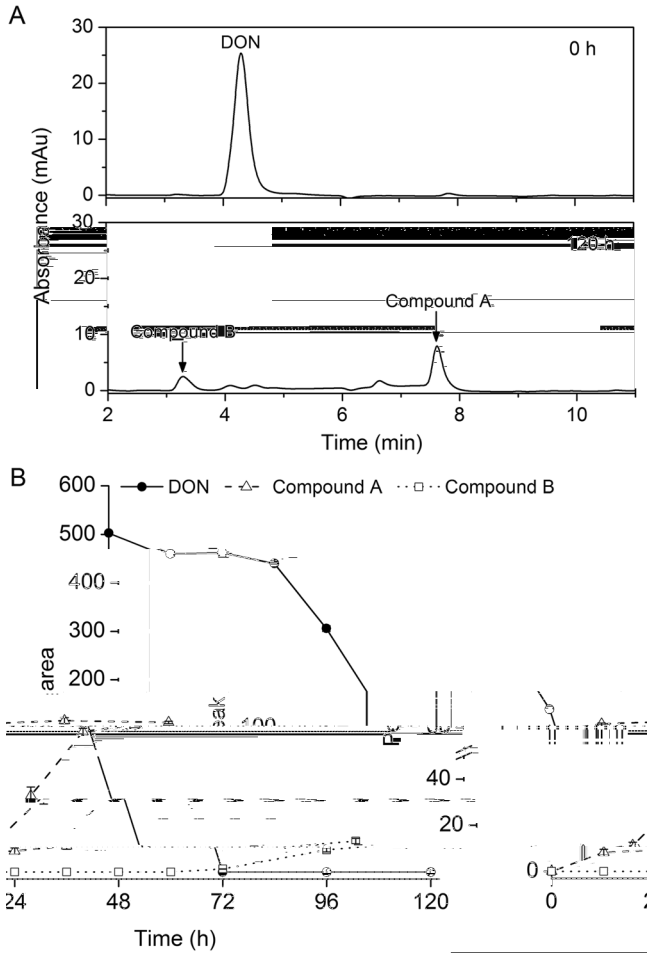

Figure 3. Chemical determination of DON and the products of DON catabolism in strain S3-4. (**A**) S3-4 was grown in mineral salts medium containing DON (100 µg/mL) and HPLC pro□les were taken at 0 h (top panel) and 120 h (bottom panel). A representative result from three independent experiments is shown. (**B**) Depletion of DON and accumulation of its catabolites under the same conditions as in Fig. 2A during a period of 120 h. □ e values given are the means of three biological replicates. □ e error bars represent the standard deviation.

and the molecular mass of the trimethysilyl group is 72, leaving a 2 dalton di□erence between DON and compound A), and compound B is 512.2 Da (the same as DON).

These compounds were further characterized by ^{1}H nuclear magnetic resonance (NMR) spectroscopy (Supplementary Fig. S3). All NMR assignments for compounds A and B were compared with previously published NMR data for 3-oxo-DON and 3-epi-DON[11,15]. □ e NMR experimental parameters, including ^{1}H chemical shi□s, multiplicity and J-coupling constants, of compounds A and B closely match those of 3-oxo-DON and 3-epi-DON, respectively (Supplementary Table S1). GC/MS (Fig. 4) and NMR results strongly indicate that compounds A and B are 3-oxo-DON and 3-epi-DON, respectively.

Reduced impact of 3-oxo-DON and 3-epi-DON on wheat seedlings. To determine whether the two DON-degradation compounds have reduced phytotoxicity, wheat coleoptiles were inoculated with 100 µg/mL of DON, 3-oxo-DON and 3-epi-DON, respectively, and the lengths of wheat leaves and coleoptiles were measured 24 hai. As shown in Fig. 5A, there were no signi□cant di□erences in coleoptile length between the four treatments. However, DON inoculation signi□cantly reduced wheat leaf length (56%) compared with the water control, whereas 3-oxo-DON or 3-epi-DON inoculation did not signi□cantly a□ect leaf length. □ us, in wheat, both 3-oxo-DON and 3-epi-DON have no or undetectable phytotoxicity.

3-oxo-DON and 3-epi-DON have reduced impact on the expression of DON-responsive genes in wheat seedlings. We next evaluated the e□ect of DON, 3-oxo-DON and 3-epi-DON on DON-responsive gene expression in wheat seedlings at 24 hai. Five wheat marker genes known to be induced by DON were assayed by qRT-PCR. Transcript levels for all □ve genes were signi□cantly lower in 3-oxo-DON or 3-epi-DON-treated seedlings than in seedlings treated with DON, with reduction in transcript levels ranging from 2.0- to 6.6-fold (Fig. 5B). □ ese results indicate the impact of 3-oxo-DON and 3-epi-DON on gene expression is signi□cantly reduced compared with DON.

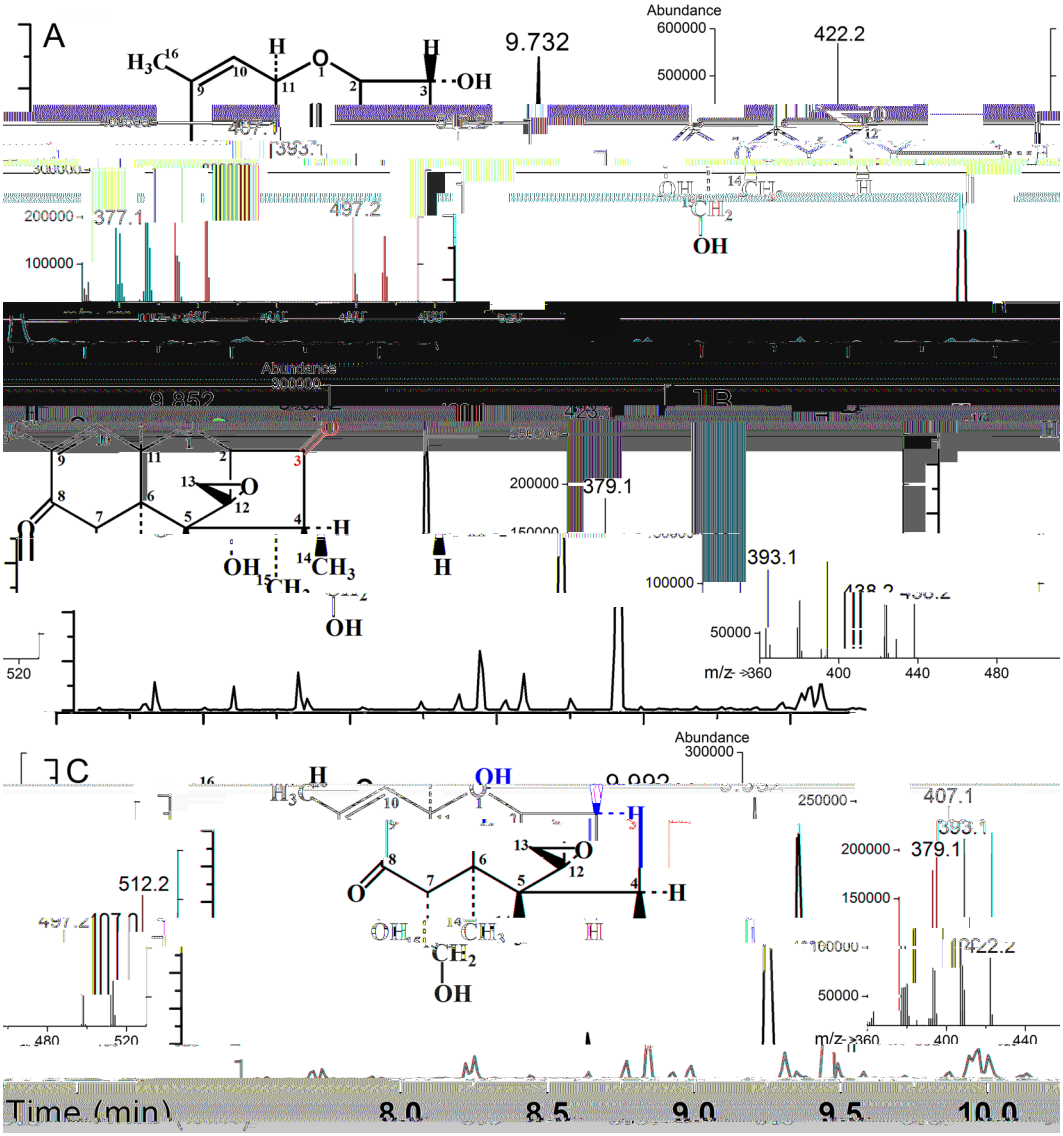

Figure 4. Gas chromatography (GC) and mass spectrometry (MS) of DON and its metabolites. (**A**) Total ion chromatogram of DON. Mass spectra for peaks representing DON are shown in the right insert. (**B**) Total ion chromatogram of compound A. Mass spectra for peaks representing compound A are shown in the right insert. (**C**) Total ion chromatogram of compound B. Mass spectra for peaks representing compound B are shown in the right insert. The structures of DON and its metabolites are shown in the le inserts.

Identification of oxidoreductase genes by comparative genomic sequence analysis. To perform comparative genome analysis with other bacteria, the S3-4 genome was sequenced. The S3-4 genome comprises three scaolds (3,153,523 bp, 1,058,422 bp and 397,147 bp in length, respectively) and two plasmids (155,520 bp and 12,966 bp in length, respectively), with a total genome size of 4.7 Mb. ere are 4,593 predicted genes, including two 5 S rRNA, two 23 S rRNA, two 16 S rRNA, and 50 tRNA genes.

The annotated protein sequence of S3-4 was compared with the genome sequences of *Devosia* sp. 17-2-E-8 (D17), which is able to degrade DON[25]. Comparative analysis revealed that 1,859 protein-coding genes are conserved between D17 and S3-4 (Fig. 6A). A second BLASTp search was conducted to compare these 1,859 proteins against the genome of *Sphingobium japonicum* UT26 (S26), which is a close relative of S3-4 but does not have DON-degrading activity[21]. is comparison revealed that 188 of the 1,895 protein-coding genes conserved between D17 and S3-4 are not present in S26 (Fig. 6A). ese 188 genes unique to the DON-degrading strains were subsequently used for identication of candidate genes responsible for DON-degradation in the S3-4 strain.

Functional annotation was done using the COG (Clusters of Orthologous Groups) database. Of the 188 unique genes, 163 could be classied into 19 functional categories (Fig. 6B). Eleven genes in the class of energy production and conversion were selected for further analysis. is class was chosen because genes responsible for energy production and conversion likely play an essential role in allowing S3-4 to grow in MM media containing DON as the only carbon source by metabolizing DON to generate energy for bacterial growth. Because

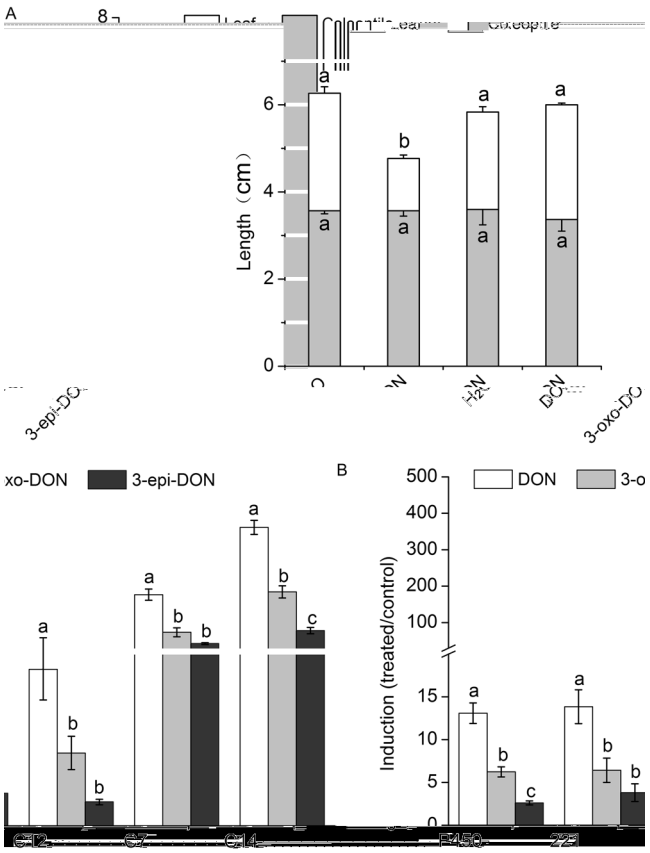

Figure 5. Toxicity of DON, 3-oxo-DON and 3-epi-DON to wheat seedlings. (**A**) The lengths of wheat leaves (white bars) and coleoptiles (gray bars) 24 hours after inoculation with DON, 3-oxo-DON, 3-epi-DON and H_2O (control). (**B**) qRT-PCR determination of the expression levels of DON-responsive genes in the wheat samples from A. The levels of gene transcripts are calculated relative to the levels in the water inoculation sample.

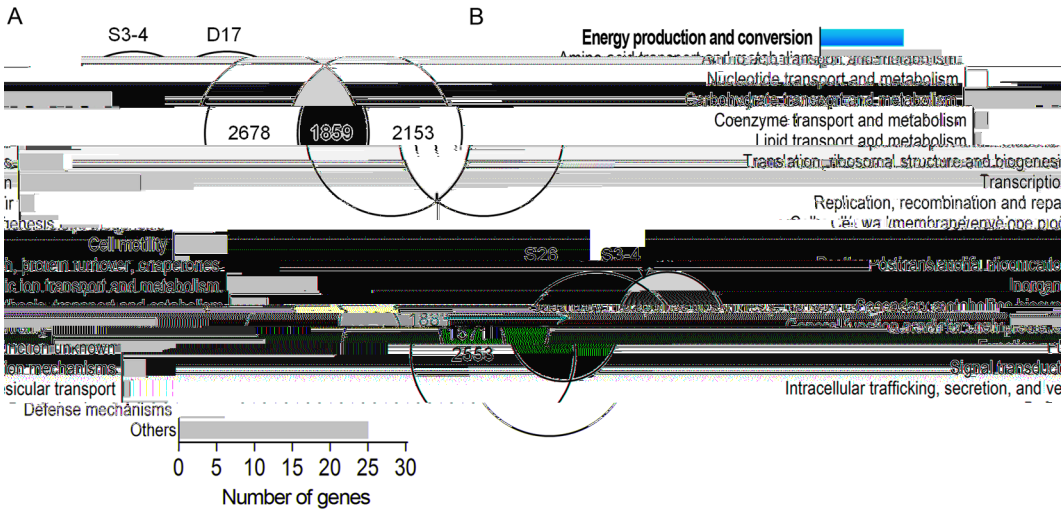

Figure 6. Candidate genes for oxidation revealed by comparative genome sequence analysis. (**A**) The Venn diagram shows comparisons of gene numbers in the *Sphingomonas* sp. strain S3-4 (S3-4), *Devosia* sp. strain 17-2-E-8 (D17) and *Sphingobium japonicum* UT26 (S26). Overlapping regions represent genes common to different genomes. (**B**) Functional classification of the genes unique to strain S3-4 according to the COG database.

the transformation of DON into 3-oxo-DON is actually the oxidation of alcohol, which may be catalyzed by a dehydrogenase, 5 of the 11 genes that encode predicted oxidoreductases (related to aryl-alcohol dehydrogenases) were considered potential DON degradation candidate genes.

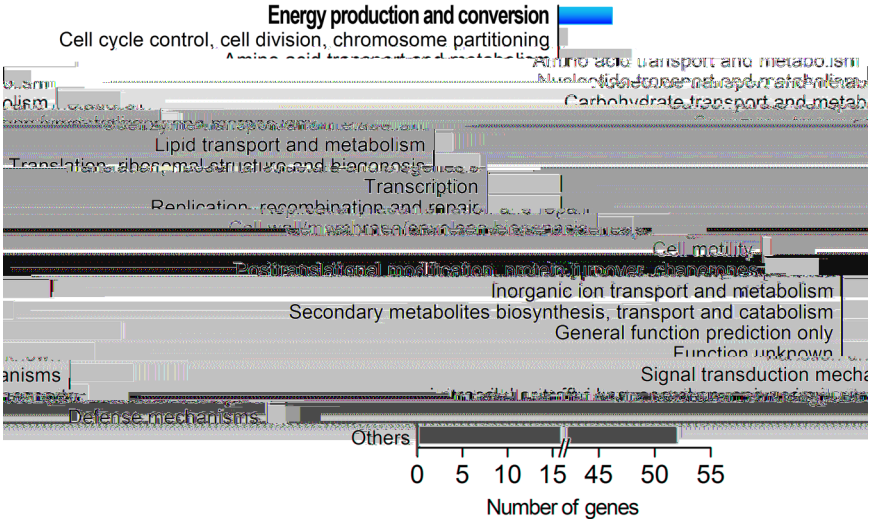

Figure 7. Functional classification of genes in one positive BAC clone isolated by functional screening. Genes functions were classified according to the COG database.

Identification of an oxidoreductase gene by functionally screening a BAC library. To identify the gene responsible for DON-degradation, a S3-4 BAC library was screened for enzymatic activity. The library consists of 2,304 clones that were arrayed in six 384-well plates. Analysis of 30 random BAC clones showed that the library had an average insert size of 120 kb with a size range from 20 to 227.5 kb and an empty-vector rate of lower than 5% (Supplementary Fig. S4). The genome coverage of this library is estimated to be more than 50-fold (based on a genome size of 4.7 Mb). When this BAC library was screened for DON-degrading activity, one positive clone was identified. The insert of this clone was 148 kb in length and contained 152 genes. These genes can be classified into 20 categories based on COG database annotation, with 6 genes belonging to the energy production and conversion category (Fig. 7). One of these genes, which was also identified as a gene unique to S3-4 and D17, encodes a predicted oxidoreductase, designated A1 (GenBank accession number: MF314460). This oxidoreductase gene is one of the five predicted oxidoreductases that were identified by comparative genomic sequence analysis (Fig. 6B) and was then further characterized.

A new aldo/keto reductase family member AKR18A1 is responsible for DON-degradation. Alignment of the amino acid sequences of the S3-4 A1 protein and aldo/keto reductases retrieved from BLAST searches showed that the A1 protein contains typical AKR signature motifs, such as an $(\alpha/\beta)_8$-barrel motif and catalytic tetrad (Asp-57, Tyr-62, Lys-90, and His-131), which are conserved among aldo-keto reductases (Supplementary Fig. S5). The AKR superfamily comprises 17 families, with more than 190 members (as of July 2015, http://www.med.upenn.edu/akr/). No AKR protein has more than 40% amino acid sequence identity to the A1 protein. A phylogenetic tree was generated based on amino acid sequence alignments of all 24 annotated AKRs from bacteria (http://www.med.upenn.edu/akr/) and the A1 protein. Based on this tree, A1 is most closely related to AKR12, but only has 37%, 36% and 35% identity to AKR12A1, AKR12B1 and AKR12C1, respectively (Supplementary Fig. S6). The nomenclature criterion for the AKR family is >40% identity[26]; therefore, these results led us to propose a new AKR family, family 18, and A1, designated AKR18A1, as the first member of this family.

Enzymatic properties of recombinant AKR18A1 expressed from *E. coli*. AKR18A1 was expressed in *E. coli* BL21, purified by affinity-chromatography and assayed for its DON-degrading activity and enzymatic properties. This recombinant protein had the expected size based on SDS-polyacrylamide gel electrophoresis (Fig. 8A) and was used in all enzymatic activity assays. The recombinant AKR18A1 protein oxidized DON to form 3-oxo-DON in the presence of cofactor $NADP^+$ (Fig. 8B), whereas no activity was seen in the presence of NAD^+ (data not shown), indicating that $NADP^+$ is essential for DON-degradation activity. The AKR18A1 protein catalyzed a reverse reaction of 3-oxo-DON into DON in the presence of the cofactor NADH (Supplementary Fig. S7), whereas no activity was seen in the presence of NADPH (data not shown).

Recombinant AKR18A1 had the highest activity at pH 10.6 and 45 °C, and activity was maintained over a wide range of pH values (from 7 to 11) and temperatures (from 10 to 50 °C), implying high stability and activity under different conditions (Fig. 8C). Km and Vmax values for AKR18A1 were 1214.4 ± 73.3 μM and 25.7 ± 0.8 nmol·min^{-1}·mg^{-1} protein, respectively (Fig. 8D), and for the cofactor $NADP^+$ in the oxidation reaction, the Km and Vmax values were 480 ± 70 μM and 53.7 ± 2.4 nmol·min^{-1}·mg^{-1} protein, respectively. Regarding reversible reduction reaction from 3-oxo-DON into DON, the Km and Vmax values for AKR18A1 were 547.1 ± 121.4 μM and 176.1 ± 19.5 nmol·min^{-1}·mg^{-1} protein, respectively, while for the cofactor NADH the Km and Vmax were 78 ± 28 mM and 147.5 ± 5.2 nmol·min^{-1}·mg^{-1} protein, respectively.

Disruption of AKR18A1 in *Sphingomonas* sp. strain S3-4. To further verify that AKR18A1 is responsible for DON-oxidation in strain S3-4, its coding sequence was disrupted by gene replacement with a disruption plasmid pK18*mobsacB*, generating an isogenic *Sphingomonas* strain, Δakr18a1, that differs from the strain S3-4 only in a single gene, *AKR18A1*. The specific disruption of *AKR18A1* was confirmed by PCR (Supplementary Fig. S8). The mutant Δakr18a1 and wild-type (WT) S3-4 strains had similar growth patterns in nutrient broth (NB) medium. When WT S3-4 was cultured in MM supplemented with 100 μg/mL DON, DON was substantially degraded at 36 hai and completely degraded at 72 hai. However, when the mutant strain Δakr18a1 was cultured under the same conditions, DON was not degraded at all during the entire culture period while the number of cells remained constant (Supplementary Fig. S9). The abolishment of DON-degrading activity in Δakr18a1 demonstrates that *AKR18A1* is the only gene responsible for oxidation of DON in S3-4.

Catabolism of zearalenone by strain S3-4 and recombinant protein AKR18A1. To determine whether AKR18A1 can target the ketone group of another *Fusarium* mycotoxin, zearalenone (ZEN), the

addition, the purified recombinant AKR18A1 protein could efficiently degrade GO and MG (Supplementary Fig. S11C and D). These results demonstrate that AKR18A1 can catabolize aldehyde compounds.

Discussion

In this study function-based screening and comparative analysis were used to isolate a DON-detoxifying bacterial strain, S3-4, and the gene responsible for catabolic activity, *AKR18A1*. Biotransformation of DON into two different compounds, 3-oxo-DON and 3-epi-DON, in the same strain provides direct evidence that DON degradation occurs via sequential reactions. To date, only two bacterial strains, one *Devosia*[10,11] and one mixed culture[14], are known to oxidize DON into 3-oxo-DON, whereas several *Devosia* and *Nocardioides* strains have been shown to epimerize DON into 3-epi-DON[10,15,27]. However, there is no a single strain that can catabolize DON into both compounds. It has been proposed that DON is first oxidized to 3-oxo-DON and then converted to 3-epi-DON[5]. In the present study we demonstrate that these reactions are sequential (Fig. 9). First, AKR18A1 catalyzes the reversible oxidation/reduction of DON to 3-oxo-DON and second, 3-oxo-DON is converted to 3-epi-DON by an unknown enzyme. In strain S3-4 there is much higher oxidation activity than epimerization activity, but the mechanistic basis for this differential activity remains unknown.

The S3-4 AKR18A1 protein contains conserved domains typical of AKR family members but is less than 40% identical to other AKR proteins. Therefore AKR18A1 represents a new member of the AKR superfamily. The AKR18A1 protein carries conserved sequences that have been identified in sequence alignments and structural analysis of AKRs. For instance, the residues of the cofactor-binding pocket across all the AKRs are strictly conserved (Asp, Asn, Gln, and Ser)[26], and these residues are all found in the AKR18A1 sequence (Asp-50, Asn-162, Gln-187, Ser-268) (Supplementary Fig. S5). The substrate-binding pocket for the AKRs is formed by the carboxyl-terminal regions of the central β-strands where there is a conserved catalytic tetrad of Tyr, Lys, His, Asp[26]. This is catalytic tetrad is also present in AKR18A1 (Supplementary Fig. S5).

The AKR18A1 protein appears to have favored catalytic direction towards the reverse reduction reaction of 3-oxo-DON into DON *in vitro* assays, whereas in the S3-4 strain, DON is completely converted into 3-oxo-DON and 3-epi-DON (Fig. 2B). This is discrepancy between recombinant the AKR18A1 protein and the S3-4 strain may relate to the presence of other proteins in the S3-4 strain that may catalyze the 3-oxo-DON to 3-epi-DON; it has been speculated that during microbial conversion from DON into 3-oxo-DON and 3-epi-DON the coupling of the transformation to another pathway may drives it away from equilibrium[26].

In addition to degrading DON, AKR18A1 catalyzes the reduction of ZEN into α-ZOL and β-ZOL (Supplementary Fig. S10), as well as the reduction of the aldehydes, GO and MG (Supplementary Fig. S11). Thus, AKR18A1 can catalyze the reduction of a wide range of ketones and/or aldehyde-containing compounds and the oxidation of alcohols. It is likely that AKR18A1 could reduce aflatoxin dialdehyde to mono and bis-alcohols, as has been demonstrated for the AKR superfamily members AKR7A2 and 7A3. This is reaction can prevent aldehydes

S3-4 within 72 h (Fig. 2), indicating the great practical potential of S3-4 in decontaminating food/feed stu. A large-scale culture of this strain via fermentation and its application for detoxi cation of DON-contaminated food/feed products are in progress. e recombinant AKR18A1 protein can also be used to detoxify DON. Moreover, because DON is a virulence factor that is required for the spread of plant FHB pathogens[1], the *AKR18A1* gene can potentially be used to control plant diseases caused by DON-producing pathogens. e improvement of plant resistance against *Fusarium* pathogens and mycotoxins is a major challenge because most cultivars currently grown are susceptible to this disease and no highly resistant germplasm is available. us the identi cation of new genes to control *Fusarium* mycotoxins, such as *AKR18A1*, is particularly important.

Conclusion

In the present study a bacterial strain, S3-4, capable of detoxifying *Fusarium* toxins was isolated and the gene responsible for detoxi cation, *AKR18A1*, was cloned. Both the S3-4 strain and the recombinant AKR18A1 protein could be used as detoxifying agents to control FHB pathogens and to reduce mycotoxin levels in food and feed products. ese results serve as the basis for future isolation of novel genes that detoxify mycotoxins and dissection of the complete pathway for degradation of *Fusarium* toxins via oxidation and epimerization.

Materials and Methods

bacterial suspension of *Sphingomonas* sp. S3-4 (1×10^{10} CFU mL^{-1}) or MM and incubated at 28 °C for 72 h in an aerobic chamber. The samples were freeze-dried. DON was extracted and assayed by HPLC as described above.

Inoculation of wheat seedlings with DON and quantitative real-time PCR. Wheat seedlings were inoculated with DON and its metabolites as described[29] and seedling lengths were scored 24 h after inoculation. Total RNA from wheat seedlings that were harvested 24 hai were used for reverse transcription and quantitative real-time PCR as previously described[29]. Five genes, P450 (cytochrome P450), 221 (Efflux family protein), C12 (Glutathione S-transferase), C7 (methionyl-tRNA synthetase) and C14 (Putative kinase), which are induced in wheat in response to DON[30], were quantitatively assayed. Primers are listed in Table S2.

BAC library construction. A BAC vector was prepared with *Hin*d III (Fermentas, MA, USA) from the high-copy composite vector pHZAUBAC1 and was used for construction of a BAC library with *Hin*d III digested genomic DNA isolated from strain S3-4 as previously described[31]. One mL overnight culture for each BAC clone was suspended in 1 mL MM containing DON (20 µg/mL). After incubation for 5 days at 37 °C, metabolites were extracted and analyzed by HPLC. The positive clone was sequenced at both ends by BGI (Shenzhen, China) with primers listed in Table S2.

Sequencing, assembly, annotation, and genome comparisons. Bacterial DNA was isolated using a DNA extraction kit (Axygen, Hangzhou, China). The genome of strain S3-4 was sequenced by Personalbio (Shanghai, China) using an Illumina Miseq system. A combination of three libraries containing 450 bp (paired-end), 3 kb and 8 kb (mate-paired) inserts was sequenced. The generated sequences were assembled using Newbler de novo (version 2.6)[32], and the pre-assembled contigs were scaffolded using the SSPACE program[33]. Gaps between contigs were closed using GapCloser software (version 1.12; http://soap.genomics.org.cn) and PCR amplification. Prediction of open reading frames (ORFs) was accomplished using Glimmer 3.0 (http://www.cbcb.umd.edu/software/glimmer/), whereas RNAmmer 1.2[34] and tRNAscan-SE (Version 1.3.1)[35] were used for the identification of rRNA and tRNA. Functional annotation of genes was done using BLAST2GO software[36] and the refseq-protein database (https://www.ncbi.nlm.nih.gov/refseq/). A putative function was assigned to each gene using a cutoff E-value of $\leq 1\ E^{-06}$. Predicted protein sequences of strains with and without DON-degradation activity, *Devosia* sp. 17-2-E-8[25] and *Sphingobium japonicum* UT26[21], respectively, were compared with strain S3-4 using bidirectional BLASTp comparisons with an E value cutoff of 10^{-5} as previously described[37].

Cloning, expression and purification of recombinant protein in *E. coli*. The *AKR18A1* gene was amplified by PCR from genomic DNA of strain S3-4 using KOD-plus-DNA polymerase (Toyobo, Shanghai, China) with the primers listed in Table S2. The PCR products were cloned into a pET-22b vector (Novagen, CA,

protein was induced by the addition of 0.2 mM IPTG. After 60 min 10 mL aliquots were exposed to a 2 mM concentration of GO or MG, and OD_{600} was determined over the course of 4 h.

GO and MG catabolism by recombinant AKR18A1 protein. The GO and MG catabolic activity of AKR18A1 was measured in a 50 µL mixture containing 100 µM each substrate, 0.2 mM NADPH and 6 µg purified protein. The reaction was terminated as described above, and substrate concentration was determined by HPLC as previously described[42].

Statistical analysis. All assays were performed in triplicate. The results were analyzed using ANOVA for multiple comparisons followed by the Duncan test using SAS software v.8.1 (SAS institute, Cary, NC, USA), with significance levels of 0.01.

References

1. Bai, G. & Shaner, G. Management and resistance in wheat and barley to *Fusarium* head blight. *Annu. Rev. Phytopathol.* **42**, 135–161 (2004).
2. Zhang, J. B. *et al*. Natural occurrence of *Fusarium* head blight, mycotoxins and mycotoxin-producing isolates of *Fusarium* in commercial fields of wheat in Hubei. *Plant Pathol.* **62**, 92–102 (2013).
3. Pestka, J. J. Deoxynivalenol: mechanisms of action, human exposure, and toxicological relevance. *Arch. Toxicol.* **84**, 663–679 (2010).
4. He, J. W., Zhou, T., Young, J. C., Boland, G. J. & Scott, P. M. Chemical and biological transformations for detoxification of trichothecene mycotoxins in human and animal food chains: a review. *Trends Food Sci. Technol.* **21**, 67–76 (2010).
5. Karlovsky, P. Biological detoxification of the mycotoxin deoxynivalenol and its use in genetically engineered crops and feed additives. *Appl. Environ. Microbiol.* **91**, 491–504 (2011).
6. Fuchs, E., Binder, E. M., Heidler, D. & Krska, R. Structural characterization of metabolites after the microbial degradation of type A trichothecenes by the bacterial strain BBSH 797. *Food Addit. Contam.* **19**, 379–386 (2002).
7. Islam, R., Zhou, T., Young, J. C., Goodwin, P. H. & Pauls, K. P. Aerobic and anaerobic de-epoxydation of mycotoxin deoxynivalenol by bacteria originating from agricultural soil. *World J. Microbiol. Biotechnol.* **28**, 7–13 (2012).
8. Ito, M. *et al*. A novel actinomycete derived from wheat heads degrades deoxynivalenol in the grain of wheat and barley affected by *Fusarium* head blight. *Appl. Microbiol. Biotechnol.* **96**, 1059–1070 (2012).
9. He, W. J. *et al*. Aerobic de-epoxydation of trichothecene mycotoxins by a soil bacterial consortium isolated using *in situ* soil enrichment. *Toxins* **8**, 277, doi:10.3390/toxins8100277 (2016).
10. Sato, I. *et al*. Thirteen novel deoxynivalenol-degrading bacteria are classified within two genera with distinct degradation mechanisms. *FEMS Microbiol. Lett.* **327**, 110–117 (2012).
11. Shima, J. *et al*. Novel detoxification of the trichothecene mycotoxin deoxynivalenol by a soil bacterium isolated by enrichment culture. *Appl. Environ. Microbiol.* **63**, 3825–3830 (1997).
12. He, J. W. *et al*. Toxicology of 3-epi-deoxynivalenol, a deoxynivalenol-transformation product by *Devosia mutans* 17-2-E-8. *Food Chem. Toxicol.* **84**, 250–259 (2015).
13. Pierron, A. *et al*. Microbial biotransformation of DON: molecular basis for reduced toxicity. *Sci. Rep.* **6**, 29105, doi:10.1038/srep29105 (2016).
14. Völkl, A., Vogler, B., Schollenberger, M. & Karlovsky, P. Microbial detoxification of mycotoxin deoxynivalenol. *J. Basic Microbiol.* **44**, 147–156 (2004).
15. Ikunaga, Y. *et al*. *Nocardioides* sp. strain WSN05-2, isolated from a wheat field, degrades deoxynivalenol, producing the novel intermediate 3-epi-deoxynivalenol. *Appl. Microbiol. Biotechnol.* **89**, 419–427 (2011).
16. Xu, J. H. *et al*. Enzymatic characteristics of 3-Acetyl deoxynivalenol oxidase by *Devosia* sp. DDS-1. *Sci. Agri. Sin.* **46**, 2240–2248 (2013).
17. Aylward, F. O. *et al*. Comparison of 26 sphingomonad genomes reveals diverse environmental adaptations and biodegradative capabilities. *Appl. Environ. Microbiol.* **79**, 3724–3733 (2013).
18. Keum, Y. S., Lee, Y. J. & Kim, J. H. Metabolism of nitrodiphenyl ether herbicides by dioxin-degrading bacterium *Sphingomonas wittichii* RW1. *J. Agric. Food Chem.* **56**, 9146–9151 (2008).
19. Manickam, N., Reddy, M. K., Saini, H. S. & Shanker, R. Isolation of hexachlorocyclohexane-degrading *Sphingomonas* sp. by dehalogenase assay and characterization of genes involved in gamma-HCH degradation. *J. Appl. Microbiol.* **104**, 952–960 (2008).
20. Peng, R. H. *et al*. Microbial biodegradation of polyaromatic hydrocarbons. *FEMS Microbiol. Rev.* **32**, 927–955 (2008).
21. Ito, M. *et al*. Bacterial cytochrome P450 system catabolizing the *Fusarium* toxin deoxynivalenol. *Appl. Environ. Microbiol.* **79**, 1619–1628 (2013).
22. Penning, T. M. The aldo-keto reductases (AKRs): Overview. *Chem. Biol. Interact.* **234**, 236–246 (2015).
23. Knight, L. P., Primiano, T., Groopman, J. D., Kensler, T. W. & Sutter, T. R. cDNA cloning, expression and activity of a second human aflatoxin B1-metabolizing member of the aldo-keto reductase superfamily, AKR7A3. *Carcinogenesis* **20**, 1215–1223 (1999).
24. Gou, X. W., Fernando, W. G. D. & Seow-Brock, H. Y. Population structure, chemotype diversity, and potential chemotype shifting of *Fusarium graminearum* in wheat fields of Manitoba. *Plant Dis.* **92**, 756–762 (2008).
25. Hassan, Y. I., Lepp, D., He, J. & Zhou, T. Draft genome sequences of *Devosia* sp. strain 17-2-E-8 and *Devosia ribo avina* strain IFO13584. *Genome Announc.* **2**, doi:10.1128/genomeA.00994-14 (2014).
26. Jez, J. M., Flynn, T. G. & Penning, T. M. A new nomenclature for the aldo-keto reductase superfamily. *Biochem. Pharmacol.* **54**, 639–647 (1997).
27. He, J. W. *et al*. Bacterial epimerization as a route for deoxynivalenol detoxification: the influence of growth and environmental conditions. *Front. Microbiol* **7**, doi:10.3389/fmicb.2016.00572 (2016).
28. Poppenberger, B. *et al*. Detoxification of the *Fusarium* mycotoxin deoxynivalenol by a UDP-glucosyltransferase from *Arabidopsis thaliana*. *J. Biol. Chem.* **278**, 47905–47914 (2003).
29. Li, X. *et al*. Resistance to *Fusarium* head blight and seedling blight in wheat is associated with activation of a cytochrome p450 gene. *Phytopathology* **100**, 183–191 (2010).
30. Zuo, D. Y. Cloning and functional characterization of genes induced by deoxynivalenol mycotoxin. Doctoral Dissertation, Huazhong Agricutural University, China, p.100 (2016).
31. Wang, X. *et al*. A BAC based physical map and genome survey of the rice false smut fungus *Villosiclava virens*. *BMC genomics* **14**, 883, doi:10.1186/1471-2164-14-883 (2013).
32. Margulies, M. *et al*. Genome sequencing in microfabricated high-density picolitre reactors. *Nature* **437**, 376–380 (2005).
33. Boetzer, M., Henkel, C. V., Jansen, H. J., Butler, D. & Pirovano, W. Scaffolding pre-assembled contigs using SSPACE. *Bioinformatics* **27**, 578–579 (2011).
34. Lagesen, K. *et al*. RNAmmer: consistent and rapid annotation of ribosomal RNA genes. *Nucleic Acids Res.* **35**, 3100–3108 (2007).
35. Lowe, T. M. & Eddy, S. R. tRNAscan-SE: a program for improved detection of transfer RNA genes in genomic sequence. *Nucleic Acids Res.* **25**, 955–964 (1997).

36. Conesa, A. *et al*. Blast2GO: a universal tool for annotation, visualization and analysis in functional genomics research. *Bioinformatics* **21**, 3674–3676 (2005).
37. Schmeisser, C. *et al*. *Rhizobium* sp. strain NGR234 possesses a remarkable number of secretion systems. *Appl. Environ. Microbiol.* **75**, 4035–4045 (2009).
38. Xue, S. *et al*. Chicken single-chain antibody fused to alkaline phosphatase detects *Aspergillus* pathogens and their presence in natural samples by direct sandwich enzyme-linked immunosorbent assay. *Anal. Chem.* **85**, 10992–10999 (2015).
39. Schäfer, A. *et al*. Small mobilizable multi-purpose cloning vectors derived from the *Escherichia coli* plasmids pK18 and pK19: selection of de□ned deletions in the chromosome of Corynebacterium glutamicum. *Gene* **145**, 69–73 (1994).
40. Kaczmarczyk, A., Vorholt, J. A. & Francez-Charlot, A. Markerless gene deletion system for sphingomonads. *Appl. Environ. Microbiol.* **78**, 3774–3777 (2012).
41. Grant, A. W., Steel, G., Waugh, H. & Ellis, E. M. A novel aldo-keto reductase from *Escherichia coli* can increase resistance to methylglyoxal toxicity. *FEMS Microbiol. Lett.* **218**, 93–99 (2003).
42. Yadav, S. K., Singla-Pareek, S. L., Ray, M., Reddy, M. K. & Sopory, S. K